A Conformational Two-State Peptide Model System Containing an Ultrafast but Soft Light Switch

Markus Löweneck,* Alexander G. Milbradt,* Christopher Root,† Helmut Satzger,† Wolfgang Zinth,† Luis Moroder,* and Christian Renner*†‡

*Max-Planck-Institut für Biochemie, 82152 Martinsried, Germany; †Lehrstuhl für Biomolekulare Optik, Ludwig-Maximilians-Universität, 80538 Munich, Germany; and ‡School of Biomedical and Natural Sciences, Nottingham Trent University, Nottingham NG11 8NS, England

ABSTRACT Combining an azobenzene chromophore with the bis-cysteinyl active-site sequence of the protein disulfide isomerase (PDI) we constructed a simple but promising model for allosteric conformational rearrangements. Paralleling cellular signaling events, an external trigger, here absorption of a photon, leads to a structural change in one part of the molecule, namely the azobenzene-based chromophore. The change in geometry translates to the effector site, in our case the peptide sequence, where it modifies covalent and nonbonded interactions and thus leads to a conformational rearrangement. NMR spectroscopy showed that the *trans*-azo and *cis*-azo isomer of the cyclic PDI peptide exhibit different, but well-defined structures when the two cystine residues form a disulfide bridge. Without this intramolecular cross-link conformationally more variable structural ensembles are obtained that again differ for the two isomeric states. Ultrafast UV/Vis spectroscopy confirmed that the rapid isomerization of azobenzene is not significantly slowed down when incorporated into the cyclic peptides, although the amplitudes of ballistic and diffusive pathways are changed. The observation that most of the energy of an absorbed photon is dissipated to the solvent in the first few picoseconds when the actual azo-isomerization takes place is important. The conformational rearrangement is weakly driven due to the absence of appreciable excess energy and can be described as biased diffusion similar to natural processes.

INTRODUCTION

Proteins determine our life. Proper operation of our body and mind is based on functional proteins. Malfunction leads to illness, if not death (1). Protein function is intimately connected to and based on protein structure and dynamics. Therefore, the problem of protein folding, still unresolved as it is, remains a major challenge in the life sciences. Although sample proteins have been studied in great depth and can possibly be considered as well understood, general rules have mostly been deduced from systematic studies of suitable model systems. For time-resolved studies, and thus direct observations of protein folding, triggers are required that initiate the folding process in a controlled and defined manner (2). Whereas modifications of solution conditions, such as pH, salt concentrations or denaturants are generally limited to timescales slower than microseconds, temperature-jump techniques can explore the nanosecond time regime. However, the fastest and most immediate way is direct excitation by light, which offers a time resolution limited only by the respective chromophore. We have demonstrated recently that very fast conformational dynamics can be elicited and monitored in an azobenzene-containing peptide model system with ultrafast pump-probe spectroscopy in the ultraviolet/visible (UV/Vis) and infrared (IR) region (3–6). These small peptide models comprised a stretch of eight amino acid residues containing the active site of the protein thioredoxin reductase (TRR) that naturally folds as part of a helix. The peptide sequence was backbone cyclized via suitable azobenzene derivatives, which act as ultrafast photo triggers. Comparison of ultrafast UV/Vis spectroscopy of the light switch with extensive computer simulations and time-resolved IR measurements showed that the initial hot and strongly driven phase of the isomerization is completed within 10 ps, whereas the weakly driven conformational rearrangements are much slower (3–6). Depending on the isomeric state of the azobenzene moiety, different conformational preferences were observed for the peptide backbones (7–9). Whereas the *cis*-azo isomers exhibited a quite diverse ensemble of structures as mimic of the unfolded state, the *trans*–azo isomers displayed reasonably well-defined geometries like a folded state (10). Despite their small size, the model systems demonstrated complex conformational dynamics on timescales of picoseconds, nanoseconds, and even longer (4). The unique advantage of these photo-responsive peptides is that they are equally accessible to experiment and theory. In fact, a remarkable agreement between theoretical modeling and spectroscopic experiment has been observed for the peptide conformational dynamics (3).

Whereas these previous peptide systems were models of fast elementary processes in protein folding, we present here a new peptide model that addresses protein dynamics. Two fundamentally different kinds of dynamics have to be distinguished. Equilibrium dynamics are thermal fluctuations that often contribute decisively to protein stability or to the ability of a protein to interact with a ligand or partner protein.

Submitted May 29, 2005, and accepted for publication December 5, 2005.

Address reprint requests to Dr. Christian Renner, School of Biomedical and Natural Sciences, Nottingham Trent University, Clifton Lane, Nottingham NG11 8NS, UK. Tel.: 44-115-848-3522; Fax: 44-115-848-6636; E-mail: christian.renner@ntu.ac.uk.

0006-3495/06/03/2099/10 $2.00

doi: 10.1529/biophysj.105.067363

The entropic contribution to the total free energy from these dynamics seems to allow fine-tuning of intra- and intermolecular interactions that can be measured by NMR or calorimetry in the case of ligand binding or denaturation/unfolding transitions and can be predicted by computer simulations. Nonequilibrium dynamics, on the other hand, are involved in all signaling processes, where receptor proteins generate a signal as response to an external stimulus. Numerous signaling pathways with a vast number of participating proteins are known, but the structural and physical basis of these processes, so far, is poorly understood. In our small and simple model system the stimulus derives from isomerization of an azobenzene moiety that is initiated by a short laser pulse of ~100 fs duration. The geometric changes that accompany the isomerization enforce a rearrangement of the attached peptide sequence (Fig. 1) that is derived from the active site of the protein disulfide isomerase. In contrast to our previous azobenzene-containing peptides we have now, for the first time (to our knowledge) created a peptide model where both azo isomers exist in defined conformational states. We would call this a conformational two-state system reflecting the fact that the molecule can exist in two defined states that are characterized by the specific conformation of the peptide backbone. It should not be confused with the common two-state model of protein folding where the two states differ in the degree of folding with one unfolded and one folded. The so-called conformational two-state system allows time-resolved observation of the transition from a defined ''resting'' state to a defined ''active'' state in analogy to respective allosteric processes in receptor proteins. Although the model system is obviously very simple, it has the advantage of being well accessible by experiment and theory. Here we report the synthesis, conformational properties, and ultrafast dynamics of the PDI peptides with particular emphasis on the analysis of the coupling between photo-trigger and peptide portion.

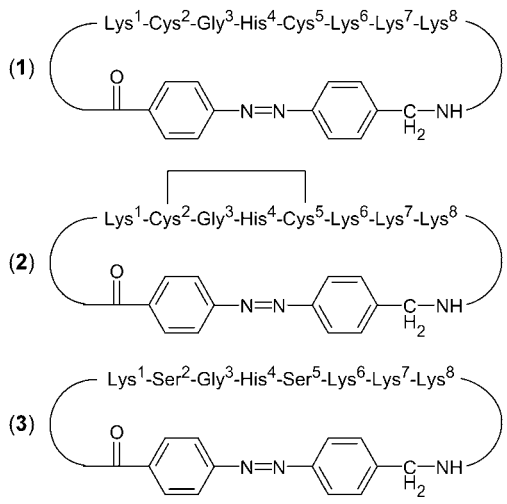

FIGURE 1 AMPB-peptides **1**–**3** containing the PDI active site motif Cys-Gly-His-Cys.

EXPERIMENTAL

Peptide synthesis

Chlorotrityl-resin was purchased from PepChem GmbH (Tübingen, Germany). All reagents and solvents used in the synthesis were of the highest quality commercially available. Fmoc-AMPB-OH was synthesized as reported previously (11). Analytical high-performance liquid chromatography (HPLC) was carried out with Waters equipments on a CC 250/4 Nucleosil 100-5 C18 column (Macherey-Nagel, Düren, Germany) using a linear gradient of CH_3CN/2% H_3PO_4 from 5:95 to 35:65 in 30 min at a flow rate of 1 ml/min. For preparative HPLC, an SP 250/10 Nucleosil 100-5 C8 HD column (Macherey-Nagel, Düren, Germany) was used with linear gradients from 0.1% TFA in H_2O (A) to 0.08% TFA in CH_3CN (B). Electron spray ionization mass spectrometry (ESI-MS) spectra were recorded on a PE Sciex API 165 spectrometer (PE Sciex, Foster City, CA). Peptide contents and concentrations were determined by UV absorption at 335 nm using an extinction coefficient of 25,000 M^{-1} cm^{-1} for the *trans*-azo isomer (11).

c[His-Cys-Lys-Lys-Lys-AMPB-Lys-Cys-Gly-]

The linear side-chain protected peptide H-His(Trt)-Cys(Trt)-Lys(Boc)-Lys(Boc)-Lys(Boc)-AMPB-Lys(Boc)-Cys(Trt)-Gly-OH was synthesized on chlorotrityl resin by standard procedures of Fmoc/tBu chemistry using HBTU/HOBt/DIEA (1:1:2) as coupling reagents. Resin detachment was carried out in HFIP/CH_2Cl_2 (1:4, v/v) and the linear side-chain protected peptide was cyclized at 2.5×10^{-4} M concentration in DMF with PyBOP/HOBt/DIEA (3 equiv; 1:1:2). To avoid partial reduction of the azo group during acidic cleavage, the resulting crude product was deprotected with TFA/H_2O (95:5, v/v) in absence of mercaptanes or trialkylsilanes as scavengers. The crude product was purified by preparative HPLC (elution with a linear gradient from 0% B to 90% B in 60 min); overall yield: 20% calculated for a peptide content of 66% (determined by UV absorption); homogeneous in HPLC: $t_R = 14.0$ min (*cis*-azo isomer) and 20.0 min (*trans*-azo isomer); ESI-MS: $m/z = 1150.6$ [M+H$^+$]; $M_r = 1149.6$ calculated for $C_{52}H_{79}N_{17}O_9S_2$.

bc[His-Cys-Lys-Lys-Lys-AMPB-Lys-Cys-Gly-]

Peptide **2** was prepared by iodine oxidation at 0.9×10^{-4} M concentration of peptide **1** in HOAc/H_2O (1:1, v/v); the crude product was purified by preparative HPLC (elution with a linear gradient from 0% B to 40% B in 60 min); yield: 28% calculated for a peptide content of 63% (determined by UV absorption); homogeneous in HPLC: $t_R = 15.3$ min (*cis*-azo isomer) and 20.7 min (*trans*-azo isomer); ESI-MS: $m/z = 1148.6$ [M+H$^+$]; $M_r = 1147.6$ calcd for $C_{52}H_{77}N_{17}O_9S_2$.

c[His-Ser-Lys-Lys-Lys-AMPB-Lys-Ser-(^{15}N)-Gly-]

Peptide **3** was prepared from the protected precursor H-His(Trt)-Ser(tBu)-Lys(Boc)-Lys(Boc)-Lys(Boc)-AMPB-Lys(Boc)-Ser(tBu)-(^{15}N)-Gly-OH as described for **1**. The glycine was labeled with the ^{15}N isotope for additional NMR analysis, which, however, proved not informative. The crude product was purified by preparative HPLC (elution with a linear gradient from 0% B to 40 B in 60 min); overall yield: 9% calculated for a peptide content of 58% (determined by UV absorption); homogeneous in HPLC: $t_R = 5.4$ min (*cis*-azo isomer) and 17.7 min (*trans*-azo isomer); ESI-MS: $m/z = 1119.8$ [M+H$^+$]; $M_r = 1118.6$ calcd for $C_{52}H_{79}N_{17}O_{11}$.

UV measurements

Stationary UV spectra were recorded on a Lambda 19 spectrometer (Perkin Elmer, Überlingen, Germany) at peptide concentrations of $2–4 \times 10^{-5}$ M in water at room temperature. The concentrations were determined by UV absorption at 335 nm using an extinction coefficient of 25,000 M^{-1} cm^{-1} (11). Thermal relaxation of peptide **3** was determined by monitoring the growth of the *trans*-azo absorption band at 335 nm. Spectra of the pure

trans-azo isomer were recorded upon relaxing the peptide over 24 h at 313 K in the dark. In the photostationary state after irradiation at 360 nm always ~20% of the *trans*-azo isomer remain. However, thermal relaxation is sufficiently slow so that the *cis*- and *trans*-azo isomer can be separated by HPLC and spectra for the pure *cis*-azo and the pure *trans*-azo peak could be obtained by the photodiode array built into the HPLC equipment. For scaling of these spectra, stationary UV spectra of the pure *trans*-azo isomer (see above) were used based on the fact that *cis*- and *trans*-azo isomer exhibit equal absorption at the isosbestic points (288 and 397 nm for both peptides **1** and **2**). The UV spectra of the pure isomers allowed us to determine that the maximum *cis*-azo content in the photostationary state is 75%–85% in agreement with NMR measurements (see below).

CD measurements

CD spectra were recorded on a JASCO (Groß-Umstadt, Germany) J-715 spectropolarimeter equipped with a thermostated cell holder and connected to a PC for signal averaging and processing. All spectra were recorded at 283 K and at peptide concentrations of 50 μM in water (pH 3.8) employing quartz cells of 1 mm optical path length. The spectra in the 190–250 nm range are reported in terms of molar ellipticity per residue $[\Theta]_R$. The concentrations were determined by UV absorption at 335 nm using an extinction coefficient of 25,000 M^{-1} cm^{-1} (11). The CD spectra of the *cis*-azo isomers were recorded after irradiation at 360 nm until the photostationary state was reached (80% ± 5% *cis*-azo isomer; see NMR measurements).

Photoisomerization

A xenon lamp 450 XBO (Osram, Munich, Germany) was used for irradiation at 360 or 430 nm (filter from Itos, Mainz, Germany) with a light intensity of ~25 mW. After irradiation the maximum *cis*- or *trans*-azo content at the photostationary state was ~80% (in both cases) as determined by ^{1}H-NMR and UV absorption measurements.

NMR spectroscopy

NMR experiments for conformational analysis of peptide **2** and **3** were carried out in water (pH 2.6) at 283 K on Bruker (Rheinstetten, Germany) DRX 500 and DMX 750 spectrometers at concentrations of 3 mM and 12 mM, respectively. The low pH was chosen to avoid chemical exchange of amide protons with water and to establish a defined protonation state for the peptide. (Note that at neutral pH the histidine residue would be partially protonated.) Additional spectra were recorded at 288 K for the *cis*-azo isomer of **3** due to resonance overlap at 283 K. Thermal *cis*→*trans* relaxation was sufficiently slow at low temperatures (Table 1) for recording the required two-dimensional (2D) data sets with high resolution also for the *cis*-azo isomer. Resonance assignments were performed according to the method of Wüthrich (12). The 2D-TOCSY spectra were recorded with spin-lock periods of 75 ms using the MLEV-17 sequence for isotropic mixing (13). Experimental rotating Overhauser enhancement (ROE) intensities were obtained from 2D-ROESY (14) experiments with mixing times of 100 ms. $^3J_{HN\text{-}H\alpha}$ coupling constants were extracted from 2D-DQF-COSY (15) and simple ^{1}H-one-dimensional (1D) spectra. All molecules were measured in a H_2O/D_2O (9:1) mixture using the WATERGATE water suppression scheme (16). Temperature shift coefficients for the amide protons were obtained from 1D and from 2D-TOCSY spectra recorded at 283, 293, and 303 K. Proton/deuterium exchange was monitored at 277 K after dissolving a lyophilized sample in D_2O on ice.

TABLE 1 Thermal relaxation of the *cis*-azo isomer to the *trans*-azo isomer for water-soluble AMPB-peptides

	Thermal relaxation k_{ct} (h^{-1})				
Compounds	283 K	293 K	303 K	313 K	E_A (kJ × mol^{-1})
PDI **2***	0.00044	0.0019	0.00672	0.0274	101
PDI **3**†	–	0.0015	0.0049	–	87.4
	280 K	295 K			
TRR bicyclic‡	–	0.0048	0.0143	0.0417	85
TRR bis-seryl‡	<0.001	0.0029	0.0080	0.0278	97

*Rates for peptide **2** were determined by NMR (see Materials and Methods).
†Rates for peptide **3** were determined by UV absorption (see Materials and Methods).
‡Previously reported rates (9).

The maximum amount of *cis*-azo isomer was obtained by recording 1D-^{1}H-NMR spectra on a sample that had been extensively irradiated. Integrals of well-separated resonances of both isomers were compared, resulting in a maximum percentage of the *cis*-azo isomer at the photostationary state of 80% ± 5% for the experimental conditions used.

The thermal *cis*→*trans* relaxation of **2** was measured at proton frequencies of 400.13 and 500.13 MHz on Bruker AMX400 and DRX500 spectrometers, respectively. After irradiation at 360 nm the sample was kept at constant temperature (±0.1 K) and permanent darkness in the magnet. Five to twenty 1D-^{1}H spectra were recorded within the approximate halftime at the respective temperature. The decay of peak heights for well-resolved signals of the *cis*-azo isomer was fit to an exponential decay curve. The activation energy was obtained from the Arrhenius plot (log $k_{c\to t}$ versus T^{-1}).

Structure calculations

The ROE intensities were converted into interproton distance constraints (**2**-*trans*: 49, **2**-*cis*: 27, **3**-*trans*: 42, **3**-*cis*: 49) using the following classification: very strong (vs) 1.7–2.3 Å, strong (s) 2.2–2.8 Å, medium (m) 2.6–3.4 Å, weak (w) 3.0–4.0 Å, very weak (vw) 3.2–4.8 Å; and the distances of pseudo atoms were corrected as described by Wüthrich (12). The $^3J_{HN\text{-}H\alpha}$ coupling constants (**2**-*trans*: 8, **2**-*cis*: 5, **3**-*trans*: 7, **3**-*cis*: 6) were converted into constraints for the backbone ϕ-dihedral angles using the Karplus relation. Multiple discrete ranges were used for the ϕ-torsion angle restraints when multiple nonoverlapping solutions existed for the Karplus equation taking into account experimental error and additional 5° uncertainty for the Karplus parameters. Distance geometry (DG) and molecular dynamics-simulated annealing (MD-SA) calculations were performed with the INSIGHTII (version 98.0) software package (Accelrys, San Diego, CA) on Silicon Graphics O2 R5000 computers (SGI, Mountain View, CA). One hundred structures were generated from the distance-bound matrices. Triangle-bound smoothing and prospective metrization were used. Embedding in three dimensions by the EMBED algorithm was followed by optimization with an SA step according to the standard protocol of the DGII package of INSIGHT II. All 100 structures were refined with a short MD-SA protocol using the DISCOVER module of INSIGHTII. After an initial minimization, 5 ps at 300 K were simulated followed by exponential cooling to ~0 K during 10 ps. A time step of 1 fs was used with the CVFF force field while simulating the solvent H_2O with a dielectric constant of 80.0. The experimental constraints were applied at every stage of the calculation with 50 kcal·mol^{-1}·$Å^{-2}$ for distance constraints and 50.0 Kcal·mol^{-1}·rad^{-2} for coupling constants. For all the selected structure ensembles no significant violations of the experimental constraints were observed.

Time-resolved UV/Vis absorption spectroscopy

The time-resolved transient absorption measurements were performed in water in the case of peptide **1**. To prevent the peptide from oxidizing, the sample solution was kept under argon atmosphere during the whole experiment. HPLC analysis after the measurements confirmed that no oxidation or degradation had taken place. The measurements on peptide **2** were done in water and DMSO. The concentrations of the peptide samples

were in all cases ~2 mM. To avoid buildup of the long-lived photoproduct, a sufficient amount of the sample (5 ml) was pumped through a quartz flow cell (optical path length of 0.5 mm). For the experiments on the *cis*-azo forms, the sample was prepared by illumination of the *trans*-azo isomer with a mercury lamp (1000 W Hg(Xe) lamp (Oriel, Darmstadt, Germany)), UG11 and WG320 (Schott, Mainz, Germany; 2 mm) filters, 120 mW in the spectral region from 320 nm to 360 nm, exposure time >2 h). The progress of the photoreaction was monitored by absorption spectroscopy. As soon as the photostationary spectrum was reached, the time-resolved transient absorption measurement was started. During this experiment, the reservoir was continuously illuminated to keep the sample in its photostationary state. Absorption spectroscopy performed on the *cis*-sample after the experiment confirmed that the photostationary state was maintained throughout the experiment.

The laser set-up consisted of a homemade Ti:sapphire CPA (chirped pulse amplifier) system, which delivered 90 fs pulses at a central wavelength of 800 nm with a repetition rate of 1 kHz and a pulse energy of 1 mJ. A small part of the fundamental light was used to generate a UV/Vis white-light continuum in a CaF_2 plate (17). For the excitation, a noncollinear optical parametric amplifier (NOPA) (18–20) was used to produce pulses at 480 nm, which were then compressed with a prism compressor to a pulse length of 80 fs. The sample was excited by the 480 nm pulse, and the transient absorption signal was measured with the UV/Vis white-light probe pulse spectrally resolved in a single shot detection set-up consisting of a photo-diode array, an amplifier, and a 96-channel analog-digital converter device (21). The irradiated volume of the sample was exchanged completely in the flow cell between two consecutive pump pulses.

Since both *cis*- and *trans*-azo isomers absorb in overlapping spectral regions, illumination is unable to produce 100% *cis*-azo samples. Only a photostationary equilibrium between *cis*- and *trans*-azo peptides with ≈75%–85% *cis*-azo molecules is reached by illumination (determined by UV and NMR, also see above). The transient absorption data were corrected for this amount of *trans*-azo molecules in the sample.

For every data point measured with a fixed delay time between pump- and probe-pulse, 20,000 single shots were averaged. The transient absorption of the solvent was subtracted from the sample signal, and the time traces at each wavelength were corrected for the corresponding chirp of the white-light continuum. For the data analysis, a global least-square fitting algorithm was used to model the data as a sum of exponential decays.

RESULTS

Peptide design and synthesis

Based on our previous experience with azobenzene-containing peptides, we chose an eight-membered peptide for backbone cyclization with the (4-aminomethyl)phenylazobenzoic acid (AMPB) chromophore. Incorporation of the Cys-Gly-His-Cys-Lys active-site motif of PDI allows for modification of the conformational restriction via formation or reduction of a disulfide bond (Fig. 1). As PDI catalyzes oxidative folding of proteins in vivo, further functional investigations can also be foreseen.

In analogy to previously reported syntheses (11), the cyclicpeptide **1** was synthesized by the Fmoc/tBu strategy on chlorotrityl-resin using the *S*-trityl group for cysteine protection. Upon cleavage from the resin by mild acid treatment, the linear precursor was cyclized in solution by the PyBOP/HOBt procedure. To avoid partial reduction of the azo group during acidic cleavage of the *S*-trityl groups, aqueous TFA was applied in absence of mercaptanes or trialkylsilanes as scavengers. Upon iodine oxidation, the bicyclic compound **2** was isolated by HPLC as homogeneous material. The reduced peptide **1** was found to be stable only for a few hours in solution due to oxidation; therefore, isosteric replacement of the cysteine residues by serine was applied in the analog **3** to allow for NMR conformational analysis of the monocyclic compound.

Photoisomerization and thermal relaxation

Cis/*trans* photoisomerization of the cyclic AMPB-peptides **1**–**3** by irradiation at 360 nm and 430 nm, respectively, is a fully reversible process with two isosbestic points at 288 and 397 nm. The UV spectra of the different peptides are virtually indistinguishable for both the *cis*- and *trans*-azo isomers. (One set of absorption curves (peptide **2**) is displayed as an *inset* in Fig. 4.) Positions and heights of the absorption peaks are very similar to previous AMPB-peptides in water (9) because chromophore and solvent are identical and only the amino acid sequence differs.

The rates of thermal relaxation ($k_{\mathrm{cis}\rightarrow\mathrm{trans}}$) of the *cis*- to the *trans*-azo ground state together with the activation energy are reported in Table 1. The activation energy is slightly smaller than for the azobenzene-peptides in DMSO (7,8) but comparable to activation energies previously observed for azobenzene-peptides in water (9), thus indicating that the peptide sequence affects only marginally the energy barrier. Whereas in the previous TRR-peptides the activation barrier is lower for the bicyclic peptide than for the monocyclic variant, possibly due to a less favorable ground state of the *cis*-azo isomer, the opposite is true for the PDI-peptides. Additional restrictions by the disulfide bridge seem to prevent the bicyclic peptide **2** from taking the easier route of the monocyclic peptide **3** from the *cis*-azo to the *trans*-azo state but require crossing of a higher energy barrier.

Circular dichroism

The circular dichroism (CD) spectra of the PDI-peptides **2** and **3** are reported in Fig. 2. Whereas the monocyclic peptide **3** exhibits a CD spectrum typical of disordered conformations with a strong negative band below 200 nm, the curves obtained for the bicyclic peptide **2** are more reminiscent of defined structures with positive signals below 200 nm and negative minima at longer wavelengths. The dichroic difference between the two isomeric forms of **3** is only in the intensity of the otherwise almost identical spectra. The more negative signal of the *cis*-azo configuration at 198 nm points to an even more disordered ensemble than for the *trans*-azo isomer. Contrarily, the positions of the minima and the wavelengths where the CD signal changes sign are very different for the two isomers of **2**. The broad minimum of the *cis*-azo isomer together with the positive maximum below 190 nm is similar in shape to spectra of helical peptides. The intensity, however, is rather weak (~25% helical conformation) and precludes the presence of a regular helix in agreement with the NMR analysis (see below). The more red

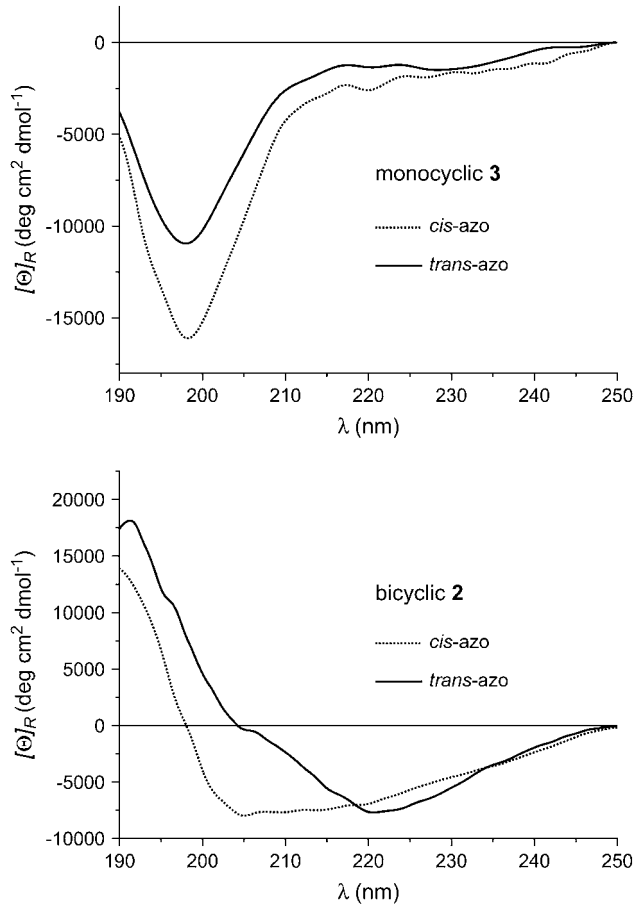

FIGURE 2 CD Spectra of azobenzene-containing PDI peptides **3** and **2**.

shifted positive maximum and the narrower minimum of the *trans*-azo isomer result in zero dichroism at 204 nm and indicate a more extended structure for the *trans*-azo isomer compared to the *cis*-azo isomer. Although contributions from irregular turns and bends as well as conformational averaging complicate interpretation of the CD spectra, good qualitative agreement with the detailed NMR conformational analysis is observed (see below).

NMR conformational analysis

The NMR spectra of the two isomers of each peptide are characterized by distinct sets of resonances. As the reduced monocyclic peptide **1** with free thiol groups was found to be stable only for a few hours at high concentrations, the serine analog **3** was used for NMR spectroscopy. Despite the presence of three adjacent lysine residues unambiguous assignment was possible even for the *cis*-azo isomer in the photostationary state. From the ROESY spectra interproton distance constraints were extracted for calculating the structural preferences of the *cis*- and *trans*-azo isomers in aqueous solution (distance constraints: **2**-*trans*: 49, **2**-*cis*: 27, **3**-*trans*: 42, **3**-*cis*: 49; ϕ-dihedral angle constraints: **2**-*trans*: 8, **2**-*cis*: 5, **3**-*trans*: 7, **3**-*cis*: 6). Table 2 summarizes statistics of the NMR constraints and of the calculations, and Fig. 3 displays the 10 lowest energy structures superimposed on backbone atoms. In contrast to all our previous azobenzene-containing peptides, well-defined conformations are observed for both isomers in the case of peptide **2**. Both isomers display a distorted β-turn for the bis-cysteinyl motif that is fixed in its geometry by the disulfide bridge. In the *cis*-azo isomer the second part of the sequence exhibits again a distorted β-turn linked to the first turn by a quite regular γ-turn centered on Cys-5 and twisted by 90° with respect to the plane of the first turn. In the *trans*-azo isomer the peptide backbone is more extended, in agreement with the analysis of the CD spectra. The γ-turn centered on Lys-5 is distorted as the three lysines are in an extended β conformation. Surprisingly, the middle lysine inserts its side chain between peptide backbone and chromophore. A flip-flop of the backbone between various conformational states, as in the case of previous azobenzene-containing peptides, could not be

TABLE 2 Statistics for the structural ensembles (10 energy lowest structures)

	2 *trans*-azo	**2** *cis*-azo	**3** *trans*-azo	**3** *cis*-azo
ROEs				
Intraresidual	3	1	0	–
Sequential	21	19	20	25
Medium range	14	5	7	15
Long range	11	2	15	9
Total	49	27	42	49
Ramachandram map				
Most favored	14%	6%	22%	0%
Additionally allowed	66%	72%	64%	94%
Generously allowed	18%	12%	8%	6%
Disallowed	2%	10%	6%	0%
Backbone root mean-square deviation (Å)	0.69	1.09	1.34	1.74
Total energy (kcal mol^{-1})	220.8 ± 4.1	225.6 ± 1.4	213.1 ± 2.9	222.2 ± 3.7
ROE violations (Å)				
Largest	0.11	0.09	0.19	0.24
Average of summed violations per structure	0.31 ± 0.06	0.21 ± 0.06	0.68 ± 0.12	0.67 ± 0.10

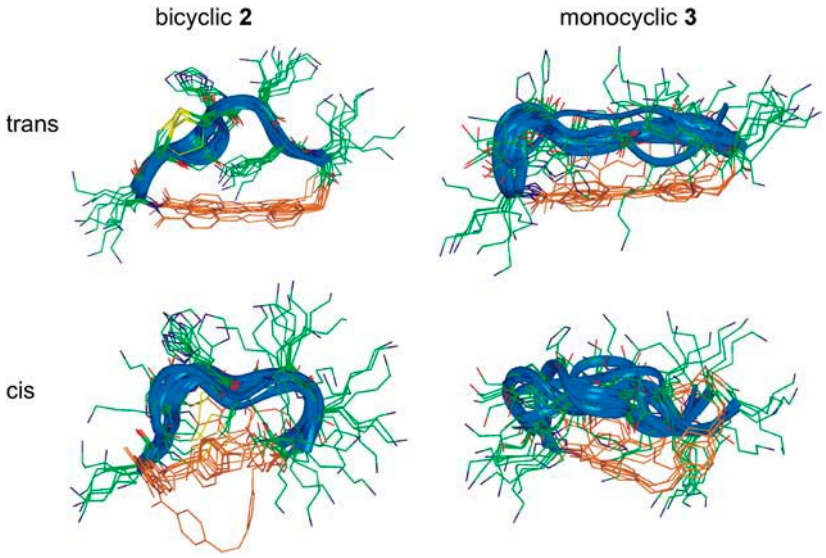

FIGURE 3 NMR structural ensembles for the *trans*-azo (*top*) and *cis*-azo (*bottom*) isomers of peptide **2** (*left*) and **3** (*right*). The 10 energy lowest structures are superimposed on backbone atoms. The chromophore is depicted in orange, and backbone conformations are highlighted by blue ribbons. Only heavy atoms are displayed.

observed, a fact that would suggest that the conformational preferences of peptide **2**, even as *cis*-azo isomer, are compatible with the constraints imposed by the bicyclic form. The analysis of ϕ- and ψ-backbone dihedral angles affords an additional and more detailed view of the backbone conformation of the peptides. Both *cis*- and *trans*-azo structural ensembles of the peptide **2** exhibit well-defined values for the backbone dihedral angles confirming the distinct conformational properties for both isomers. The irregularity of the turns expresses itself in numerical values for ϕ and ψ that show some deviation from those observed for regular β- and γ-turns. This observation is in line with an analysis of the Ramachandran map of the structures: Although few residues are outside the allowed area, most are in the additionally allowed part, not in the most favored region. The distortion of the turns together with slightly nonoptimal ϕ- and ψ-values point to a small residual tension in the bicyclic peptide. To distinguish irregularity from instability it should be emphasized that the turns as discussed above do not occur with low frequency in the calculated ensemble, but with distorted geometry. The specific nonideal geometry for a given turn is observed for all or almost all individual structures within the NMR ensemble. Although turns are not easily deduced directly from the NMR data by characteristic nuclear Overhauser effect (NOE) patterns and coupling constants (12), they are in line with our assignment of structural elements. The strongest of the nonsequential contacts for the βI-turn is the H$\alpha(i + 1)$ − HN$(i + 3)$ ROE that is indeed observed for *cis*- and *trans*-azo isomer. Relatively large $^3J_{HN\text{-}H\alpha}$ coupling constants (8.3 Hz for *cis*-azo, 8.0 Hz for *trans*-azo) come close to the ideal value of 9 Hz for the $i + 2$ position of a βI-turn (His-4 in this case), whereas for the $i + 1$ position only 4 Hz are expected (not available for *cis*-azo, 5.5 Hz for *trans*-azo). In the *cis*-azo isomer the small Hα-HN coupling of 6.0 Hz for Lys-7 is near the anticipated 5.0 Hz for residue $i + 2$ of a βII-turn. Contrarily, Lys-7 of the *trans*-azo isomer exhibits a large coupling constant of 8.5 Hz in agreement with an extended conformation.

In contrast to the defined geometry of the bicyclic peptide **2**, the monocyclic peptide **3** is more relaxed both as *cis*- and *trans*-azo isomer since pronounced conformational variability is observed in the NMR structural ensembles, both in the Cartesian coordinates (Fig. 3) and the backbone dihedral angles. The Cys-2 to Cys-5 turn of the bicyclic peptide is shifted by one amino acid in the bis-seryl analog and comprises Lys-1 to His-4 albeit in variable orientations. The second part of the sequence is even less ordered with undefined bends or turns. The *trans*-azo isomer of the bis-seryl peptide exhibits again in this part a more extended backbone than the *cis*-azo isomer. In this case cyclization of the octapeptide did not afford the expected conformational restriction. No stable hydrogen bond could be identified for any of the isomers from the H/D-exchange experiments and the temperature shifts of the amide protons. These experimental facts are well reproduced in the calculated structures that exhibit hydrogen bonding only with low frequency. For semiflexible or transiently structured peptides such as peptide **3**, the calculated NMR ensemble despite showing a diversity of conformers might still underestimate the conformational variability because the averaging properties of the NOE or ROE emphasize short distances and therefore more compact structures (22).

Ultrafast time-resolved UV/Vis absorption spectroscopy

Results from transient absorption experiments on the peptide **1** in water are shown in Fig. 4. Protecting the free thiol groups of **1** from oxidation by the argon atmosphere was sufficient for the duration of these experiments as evidenced by analytical HPLC. When the peptide in the *trans*-azo form is excited at 480 nm into the nπ*-band we observe an absorption

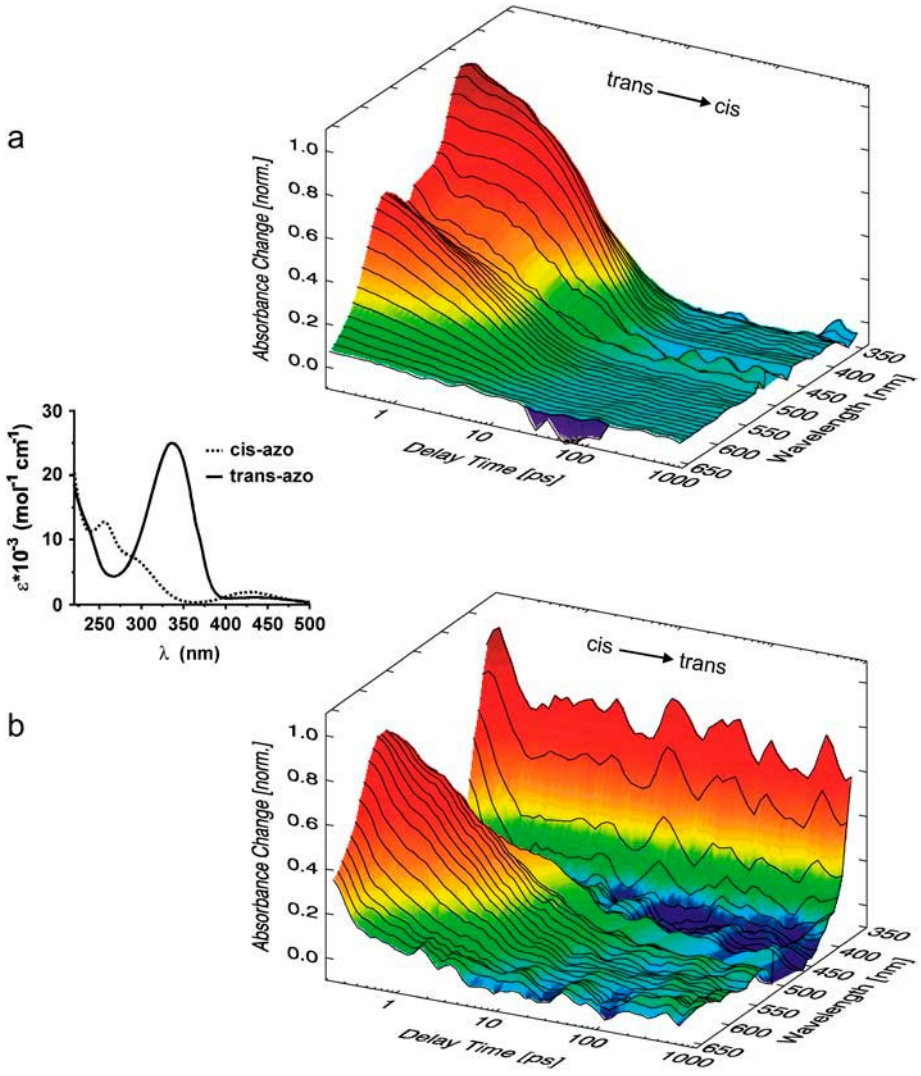

FIGURE 4 Transient absorption changes of peptide **1** for the *trans* → *cis* (*top*) and the *cis* → *trans* (*bottom*) reaction for different delay times and probing wavelengths. The white-light probe pulses covered a spectral range from 350 nm to 650 nm. The inset in the middle shows the UV absorption curve of peptide **2**.

increase throughout the visible spectral range (see Fig. 4 *a*). The absorption increase consists of two bands peaking at 560 nm and 420 nm. There is an absorption decrease around 350 nm in the vicinity of the $\pi\pi^*$ absorption band. At later times the absorption increase evolves multiexponentially: the first kinetic component is related to a weak absorption increase in the visible range, occurring with a time constant of $\tau_1 \approx$ 0.2 ps. With the second kinetic component ($\tau_2 \approx 1.2$ ps) absorption decreases around 550 nm and 390 nm, whereas a weak absorption increase occurs around 450 nm. Most of the remaining absorption difference decays with the third time constant of $\tau_3 \approx 6.6$ ps. After this time we observed negligible absorption changes in the visible part of the absorption spectra. Only in the spectral range of the $\pi\pi^*$ absorption band of *trans* isomer of peptide **1** was there a detectable absorption decrease due to the isomerized chromophores. The kinetic behavior observed for the *trans*- to *cis*-azo reaction of the cyclic PDI azobenzene peptide **1** is similar to the features observed for the cyclic azo-TRR peptides, where we had found that the isomerization of the azobenzene chromophore from *trans*- to *cis*-azo is completed within $<$10 ps (6).

When the *cis*-azo form of peptide **1** is excited at 480 nm, (Fig. 4 *b*), we observe a more structured absorption change at early delay times. There is a pronounced peak at 560 nm. The initial kinetic component ($\tau_2 \approx 0.2$ ps) has large relative amplitudes. It is connected with a strong absorption decrease in the red wing of the spectrum ($\lambda > 530$ nm) as well as around 400 nm. A second, weaker process occurring with $\tau_2 \approx 1.3$ ps is connected to a decrease and a blue shift of the 560 nm peak. The 5.8 ps kinetic component is related to a broad decrease of absorption between 400 and 600 nm. At late delay times we find an absorption change composed of a strong increase around 350 nm in the range of the $\pi\pi^*$ absorption band of *trans*-azobenzene and a weak decrease at larger wavelengths. These absorption features are similar to the difference of the equilibrium absorption spectra of the photostationary *cis*- and *trans*-azo states. By comparison with the results from azo-TRR peptides we can assign the two initial kinetic components to the isomerization of the

azobenzene chromophore and the 5 ps kinetic component to the transfer of excess energy to the surrounding solvent and the relaxation of strain on the azobenzene chromophore (3,5,6). For the initial isomerization and cooling processes the amino acid sequence seems of lesser importance in the case of the monocyclic peptides as evidenced by the close agreement of time constants for TRR- and PDI-peptides (see Table 3).

The experiments on bicyclic PDI azobenzene peptide **2** dissolved in water and DMSO qualitatively display similar absorption changes. Again these experiments exhibit three kinetic components leading to a state with modified absorption at the end of the observation time. The finally reached difference spectra are in line with the corresponding steady-state difference spectra obtained after extensive illumination. Fitting the absorption changes of the different samples with the exponential model functions, we obtain the results summarized in Table 3. The time constants are very similar for the two different peptides dissolved in H_2O. However the most pronounced differences originate from the exchange of the solvent. Whereas the two fast kinetic components remain unchanged, the slow kinetic is considerably modified. For the more viscous solvent DMSO, τ_3 is increased by 50% and 100% for the *trans*- to *cis*-azo and *cis*- to *trans*-azo reaction, respectively. Table 3 contains in parentheses the values previously obtained for the TRR-peptides. It can be seen that also for the TRR sequence the two fast kinetic components, assigned to strongly driven photochemical reactions of the chromophore azobenzene, do not depend on the solvent (6). However, the slower kinetic components—apparently due to heat dissipation to the solvent and structural changes of the peptide moiety—are faster in water than in DMSO as expected from the differences in viscosity and in heat capacity of the two solvents. For the *trans*- to *cis*-azo direction there is no marked difference between the bicyclic TRR- and PDI-peptides for any of the time constants in water or in DMSO. Only in the case of the *cis*- to *trans*-azo isomerization of the bicyclic peptides is a dependence of the kinetic behavior on the specific amino acid sequence observed (Table 3). The slow component that corresponds to the final cooling of the chromophore as well as the initial rearrangements of the peptide backbone is faster for the PDI motif compared to the oxidized TRR-peptide. This could well be explained by the pronounced conformational heterogeneity of the bicyclic *cis*-azo TRR-peptide in DMSO (8) and water (9) compared to the relatively well-defined structure of the present peptide **2**.

TABLE 3 Time constants of cyclic (1) and bicyclic (2) PDI peptides dissolved in water and DMSO

	τ_1 (ps)	τ_2 (ps)	τ_3 (ps)
Peptide **1** *trans* → *cis* in water	0.2 (0.2)	1.2 (1.3)	6.6 (6.5)
Peptide **1** *cis* → *trans* in water	0.2 (0.2)	1.3 (1.3)	5.8 (4.6)
Peptide **2** *trans* → *cis* in water	0.2 (0.2)	1.2 (1.6)	6.6 (5.8)
Peptide **2** *cis* → *trans* in water	0.2 (0.4)	1.0 (2.9)	5.6 (5.3)
Peptide **2** *trans* → *cis* in DMSO	0.2 (0.3)	1.2 (1.6)	9.8 (10.4)
Peptide **2** *cis* → *trans* in DMSO	0.2 (0.3)	1.0 (5.3)	13 (100)

For all samples, there is a long lasting absorbance change due to photoproduct formation. In parentheses, the corresponding values for the TRR peptides from Wachtveitl et al. (5) and Satzger et al. (6) are reproduced.

DISCUSSION

In our previously reported azobenzene-containing peptides, one or both isomeric states always exhibited multiple conformational families (7–9,23). These peptides were useful models for the study of fast folding/unfolding processes (3–6). Incorporation of the bis-cysteinyl PDI active-site sequence allowed now for the first time, to our knowledge, the establishment of a conformational two-state system as a simple model for allosteric structural rearrangements. Fig. 5 depicts the pronounced structural changes that result from isomerization of the azobenzene group. Whereas the Cys-Gly-His-Cys motif is kept in a similar arrangement by the disulfide bridge, the second half of the octapeptide stretch as well as the position of the AMPB moiety relative to the peptide backbone undergo major alterations. The structural transition that takes place upon isomerization from the *trans*-azo to the *cis*-azo state can be described as an almost 180° hinge motion around Cys-2/Cys-5 concomitant with a transformation of the Lys-6 to Lys-8 part from extended conformation into a βII-turn (Fig. 5). The disulfide bridge, which in the *trans*-azo isomer is rather distant from the azobenzene moiety, is brought close to the chromophore by this rotation. Although the dihedral angle of the disulfide bridge ($\pm$90°) is not defined by the experimental data, the structure calculations indicate that the preferential arrangement is different for the two isomeric states of **2**.

It should be noted that the present azo-PDI peptides differ from the former azo-TRR peptides only in the side chains of three amino acid residues and have the identical ring size.

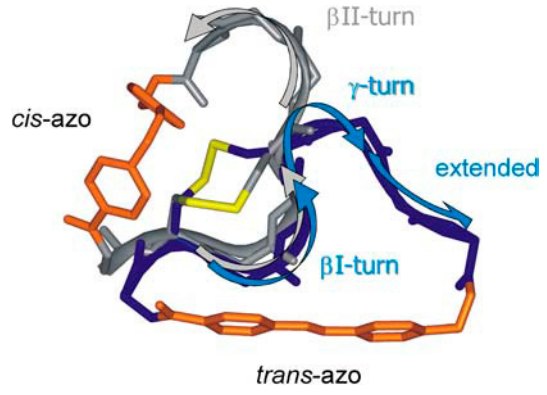

FIGURE 5 Comparison of the structure of the *cis*-azo (*gray backbone*) and *trans*-azo (*blue backbone*) isomer of the bicyclic peptide **2**. Structural elements are emphasized by arrows and labeled by type. Side chains are only shown for the cystine residues.

The replacement of Ala-3 by Gly-3 in the PDI-peptides introduces additional flexibility into the backbone, because glycine can adopt more backbone conformations than any other amino acid residue due to the lack of a side chain. The conformational constraint introduced by the backbone cyclization via AMPB is relaxed to some extent by the flexibility of the glycine, apparently allowing the formation of an energetically favorable well-defined backbone structure for the *cis*- and *trans*-azo isomer of the bicyclic peptide **2**. As expected, the change from threonine in the azo-TRR peptides to histidine in the PDI peptides does not severely affect the structural preferences, and in both cases the side chains point toward the solvent. Similarly, the replacement of aspartate by lysine is accompanied by only small differences, although these amino acids differ in their side-chain charge. Obviously, the positively charged lysine side chains are repelling each other in the azo-PDI peptides. However, even the negatively charged aspartate does not markedly interact with the following lysines in the azo-TRR peptides. Probably the entropic cost of fixing the side chains is not compensated for by the small enthalpic gain afforded by a solvent exposed salt bridge. The fact that the higher backbone flexibility of the glycine has such a significant effect on the structural preferences of the peptide is in agreement with previous studies on azobenzene-containing peptides, where introduction of a flexible methylene spacer into the chromophore completely altered the conformational behavior of the respective peptides (7,8).

The time-resolved pump-probe experiments in the UV/Vis spectral range confirm that isomerization of the azobenzene moiety in the azo-PDI peptides is completed within a few picoseconds as previously observed for the azo-TRR peptides as well as for azobenzene itself (5,24–27). Therefore, the requirement for a fast trigger for initiation of the conformational change is well met in the current model system. A second major concern is the way in which the rearrangement of the peptide backbone is driven. In naturally occurring processes the driving force for an allosteric structural change is usually not very strong. If in our peptide model the full energy of the absorbed photon ($\sim$250 kJ mol^{-1}) would be transferred to the peptide portion, little information could be derived, as in the presence of high excess energy all details of the energy landscape of the peptide would be lost. The fact that after the fast cooling phase the chromophore already exhibits the steady-state spectrum for the PDI peptides shows that the peptide does not affect the AMPB chromophore during the weakly driven slow phase. We have shown previously by comparison with elaborated MD simulations and time-resolved IR spectroscopy (3–6) that indeed the absorption characteristics of the light switch are sensitive to strain or excess energy in the peptide part. As for the TRR-peptides we find also in the case of the PDI-peptides that most of the energy that is absorbed by the chromophore is dissipated to the surrounding solvent in the first few picoseconds during the actual isomerization process. It is clear that the azo moiety cannot undergo isomerization without any movements of the remaining part of the molecule. However, MD simulations ((3) and C. Renner, unpublished work) have shown that during the ''hot'' phase of the isomerization when a lot of excess energy is still contained in the chromophore only very localized changes in the form of a few bond rotations accommodate the altered geometry, but do not significantly change the overall conformation of the peptide part. The slowest changes with appreciable amplitude in the time-resolved UV/Vis absorption spectra have time constants of $\sim$10 ps and correspond to both final cooling of the chromophore and relaxation of the joints to the peptide sequence. Only a small portion of the energy is stored in distortions of the covalent geometry and in unfavorable nonbonded interactions that subsequently drive the peptide toward the new equilibrium structure in a more diffusive-like manner. Therefore, the AMPB chromophore can be considered a soft light switch for the conformational rearrangement of the peptide sequence. The similarity of the short-time behavior of the azo-TRR peptides and the azo-PDI peptides shows that the specific amino acid sequence has little influence on the switching properties, although it obviously determines the peptide-related conformational change that is associated with the isomerization of the chromophore.

In this regard, the simple model system seems optimally suited for studying the complex relation between amino acid sequence and resultant conformational properties. Not only the stationary equilibrium structures can be investigated, but also the nonequilibrium dynamics associated with the conformational search for the structure of lowest energy. An additional advantage is the small size of the system that allows meaningful simulations by MD methods to be carried out. In fact, we have recently shown that equilibrium structures of such peptides can be correctly predicted by state-of-the-art MD combined with sophisticated data analysis (22), and promising results have also been obtained even for the nonequilibrium processes (3).

CONCLUSIONS

With the bicyclic azobenzene-peptide we succeeded in the design of a simple model system for allosteric rearrangements. In fact, NMR conformational analysis showed that the bicyclic disulfide-bridged peptide exhibits a well-defined structure in the *trans*-azo ''resting'' state as well as in the *cis*-azo ''excited'' state. Even the monocyclic variant markedly changes its structural properties upon isomerization of the chromophore although it is conformationally more variable, possibly resembling the properties of semiflexible surface loops. Ultrafast time-resolved UV/Vis spectroscopy demonstrated for both systems that isomerization of the light trigger is completed within a few picoseconds. More importantly, most of the photon energy is dissipated to the surrounding solvent, thus avoiding a nonphysiological energy overload

for the peptide part. In resemblance to typical cellular signaling events, the trigger—in the current case the photoisomerization of the chromophore—induces a change in the energy landscape of the peptide, which subsequently has to undertake a search for the new minimum-energy conformation. Future studies will investigate the time course of the light-induced peptide motion toward its new equilibrium structure by time-resolved IR spectroscopy.

SUPPLEMENTARY MATERIAL

An online supplement to this article can be found by visiting BJ Online at http://www.biophysj.org.

The study was supported by SFB 533 of the Ludwig-Maximilians-University of Munich (grants A8 and B9).

REFERENCES

1. Dobson, C. M. 2003. Protein folding and disease: a view from the first horizon symposium. *Nat. Rev. Drug Discov.* 2:154–160.
2. Volk, M. 2001. Fast initiation of peptide and protein folding processes. *Eur. J. Org. Chem.* 2001:2605–2621.
3. Spörlein, S., H. Carstens, H. Satzger, C. Renner, R. Behrendt, L. Moroder, P. Tavan, W. Zinth, and J. Wachtveitl. 2002. Ultrafast spectroscopy reveals sub-nanosecond peptide conformational dynamics and validates molecular dynamics simulation. *Proc. Natl. Acad. Sci. USA.* 99:7998–8002.
4. Bredenbeck, J., J. Helbing, A. Sieg, T. Schrader, W. Zinth, C. Renner, R. Behrendt, L. Moroder, J. Wachtveitl, and P. Hamm. 2003. Picosecond conformational transition and equilibration of a cyclic peptide. *Proc. Natl. Acad. Sci. USA.* 100:6452–6457.
5. Wachtveitl, J., S. Spörlein, H. Satzger, B. Fonrobert, C. Renner, R. Behrendt, D. Oesterhelt, L. Moroder, and W. Zinth. 2004. Ultrafast conformational dynamics in cyclic azobenzene peptides of increased flexibility. *Biophys. J.* 86:2350–2362.
6. Satzger, H., C. Root, C. Renner, R. Behrendt, L. Moroder, J. Wachtveitl, and W. Zinth. 2004. Picosecond dynamics in water soluble azobenzene-peptides. *Chem. Phys. Lett.* 396:191–197.
7. Renner, C., R. Behrendt, S. Spörlein, J. Wachtveitl, and L. Moroder. 2000a. Photomodulation of conformational states. I. Mono- and bicyclic peptides with (4-amino) phenyl azobenzoic acid as backbone constituent. *Biopolymers.* 54:489–500.
8. Renner, C., J. Cramer, R. Behrendt, and L. Moroder. 2000b. Photomodulation of conformational states. II. Mono- and bicyclic peptides with (4-amino) methyl phenyl azobenzoic acid as backbone constituent. *Biopolymers.* 54:501–514.
9. Renner, C., R. Behrendt, N. Heim, and L. Moroder. 2002. Photomodulation of conformational states. III. Water-soluble bis-cysteinyl-peptides with (4-aminomethyl) phenylazobenzoic acid as backbone constituent. *Biopolymers.* 63:382–393.
10. Behrendt, R., C. Renner, M. Schenk, F. Q. Wang, J. Wachtveitl, D. Oesterhelt, and L. Moroder. 1999a. Photomodulation of the conformation of cyclic peptides with azobenzene moieties in the peptide backbone. *Angew. Chem. Int. Ed. Engl.* 38:2771–2774.
11. Behrendt, R., M. Schenk, H.-J. Musiol, and L. Moroder. 1999b. Photomodulation of conformational states. Synthesis of cyclic peptides with backbone-azobenzene moieties. *J. Pept. Sci.* 5:519–529.
12. Wüthrich, K. 1986. NMR of Proteins and Nucleic Acids. John Wiley, New York.
13. Bax, A., and D. G. Davis. 1985a. MLEV-17 based two dimensional homonuclear magnetization transfer spectroscopy. *J. Magn. Reson.* 65:355–360.
14. Bax, A., and D. G. Davis. 1985b. Practical aspects of two-dimensional transverse NOE spectroscopy. *J. Magn. Reson.* 63:207–213.
15. Rance, M., O. W. Sorensen, G. Bodenhausen, G. Wagner, R. R. Ernst, and K. Wüthrich. 1983. Improved spectral resolution in COSY 1H NMR spectra of proteins via double quantum filtering. *Biochem. Biophys. Res. Commun.* 117:479–485.
16. Sklenar, V., M. Piotto, R. Leppik, and V. J. Saudek. 1993. Gradient-tailored water suppression for ^{1}H-^{15}N HSQC experiments optimized to retain full sensitivity. *J. Magn. Reson.* 102:241–245.
17. Huber, R., H. Satzger, W. Zinth, and J. Wachtveitl. 2001. Noncollinear optical parametric amplifiers with output parameters improved by the application of a white light continuum generated in CaF2. *Opt. Commun.* 194:443–448.
18. Wilhelm, T., J. Piel, and E. Riedle. 1997. Sub-20-fs pulses tunable across the visible from a blue-pumped single-pass noncollinear parametric converter. *Opt. Lett.* 22:1494–1497.
19. Lochbrunner, S., T. Wilhelm, J. Piel, S. Spörlein, and E. Riedle. 1999. Sub-20-fs tunable pulses in the visible and NIR by noncollinear optical parametric amplification (NOPA). *In* OSA Trends in Optics and Photonics, Vol. 26. M. M. Fejer, H. Injeyan, and U. Keller, editors. OSA, Washington, DC. 366.
20. Riedle, E., M. Beutter, J. Piel, S. Schenkl, S. Spörlein, and W. Zinth. 2000. Generation of 10 to 50 fs pulses tunable through all of the visible and the NIR. *Appl. Phys. B.* 71:457–465.
21. Seel, M., E. Wildermuth, and W. Zinth. 1997. A multichannel detection system for application in ultra-fast spectroscopy. *Meas. Sci. Technol.* 8:449–452.
22. Carstens, H., C. Renner, A. G. Milbradt, L. Moroder, and P. Tavan. 2005. Multiple loop conformations of peptides predicted by molecular dynamics simulations are compatible with NMR. *Biochemistry.* 44: 4829–4840.
23. Milbradt, A. G., M. Löweneck, S. S. Krupka, M. Reif, E.-K. Sinner, L. Moroder, and C. Renner. 2005. Photomodulation of conformational states. IV. Integrin binding rgd-peptides with (4-aminomethyl)phenylazobenzoic acid as backbone constituent. *Biopolymers.* 77:304–313.
24. Nägele, T., R. Hoche, W. Zinth, and J. Wachtveitl. 1997. Femtosecond photoisomerization of *cis*-azobenzene. *Chem. Phys. Lett.* 272:489–495.
25. Wachtveitl, J., T. Nägele, B. Puell, W. Zinth, M. Krüger, S. Rudolph-Böhner, D. Oesterhelt, and L. Moroder. 1997. Ultrafast photoisomerization of azobenzene compounds. *J. Photochem. Photobiol.* 105:283–288.
26. Satzger, H., S. Spörlein, C. Root, J. Wachtveitl, W. Zinth, and P. Gilch. 2003. Fluorescence spectra of *trans*- and *cis*-azobenzene—emission from the Franck-Condon state. *Chem. Phys. Lett.* 372:216–223.
27. Satzger, H., C. Root, and M. Braun. 2004. Excited-state dynamics of *trans*- and *cis*-azobenzene after UV excitation in the $\pi\pi^*$ band. *J. Phys. Chem. A.* 108:6265–6271.